Graphene-like metal-organic frameworks: Morphology control, optimization of thin film electrical conductivity and fast sensing applications

Supporting information

Bastian Hoppe[1*], Karen D.J. Hindricks[1*], Dawid P. Warwas[1*], Hendrik A. Schulze[1*], Alexander Mohmeyer[1*], Tim J. Pinkvos[1*], Saskia Zailskas[1*], Marc R. Krey[1*], Christopher Belke[2*], Sandra König[3], Michael Fröba[3], Rolf J. Haug[2*], Peter Behrens[1*]

[1] Institut für Anorganische Chemie, Leibniz Universität Hannover, Callinstraße 9, 30167 Hannover

[2] Institut für Festkörperphysik, Leibniz Universität Hannover, Appelstraße 2, 30167 Hannover

3 Institut für Anorganische und Angewandte Chemie, Universität Hamburg, Martin-Luther-King-Platz 6, 20146 Hamburg

[*] Laboratory of Nano and Quantum Engineering (LNQE), Leibniz Universität Hannover, Schneiderberg 39, 30167 Hannover

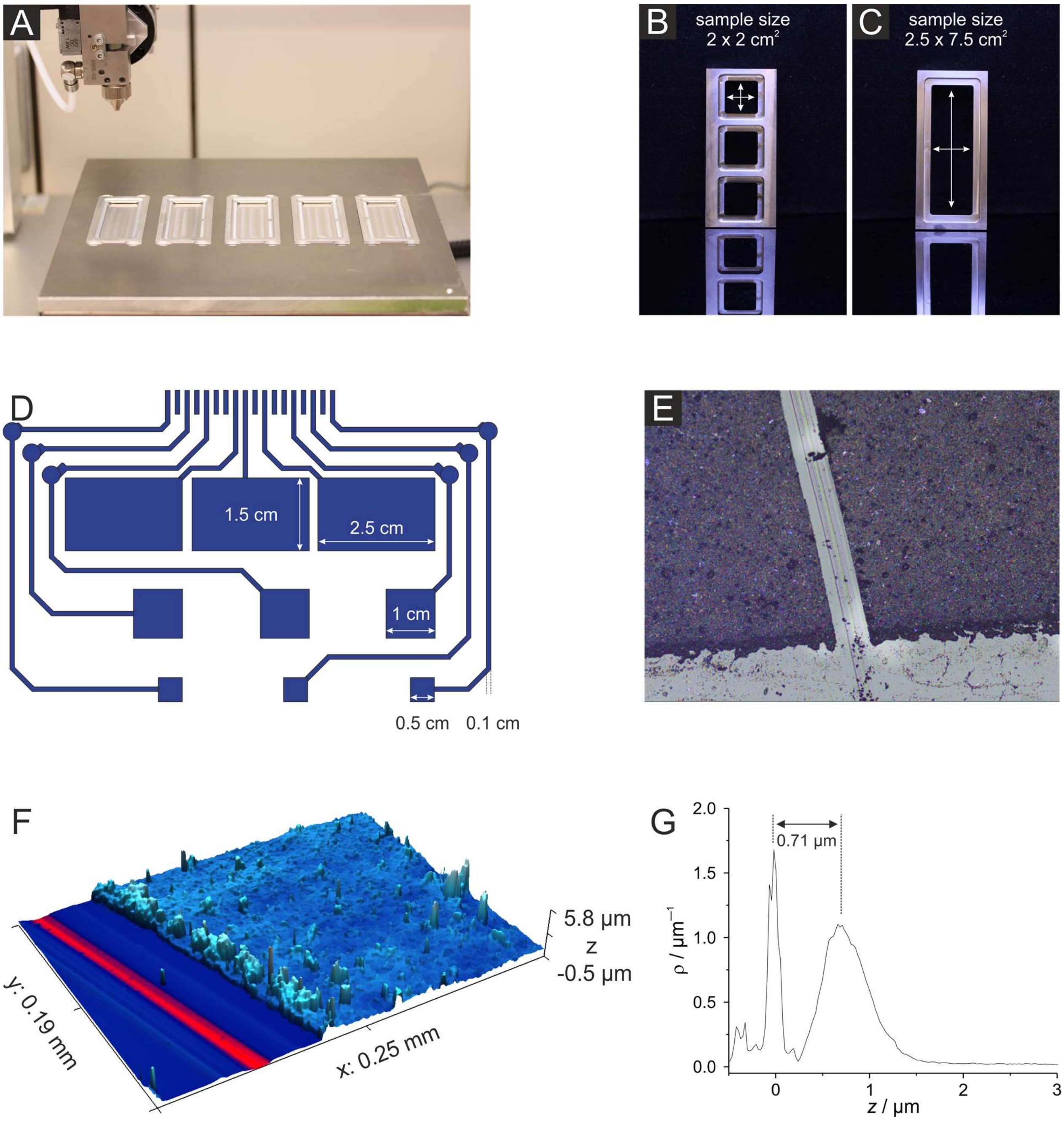

SI Fig. 1: A) Setup used for automated spray-coating; 5 samples can be coated at the same time. B) Mask used for coatings on glass slides. C) Mask used for coatings on polycarbonate foils. D) Scheme of switchboard circuit with size of the components. E) Digital image at the edge of a conducting pathway. The scratch is used for height determination. F) Topographic image by confocal microscopy. The area in dark blue represents the height of the polycarbonate foil, the light blue area represents the coating. G) Height distribution of the topographic image in D; a thickness of 710 nm can be determined.

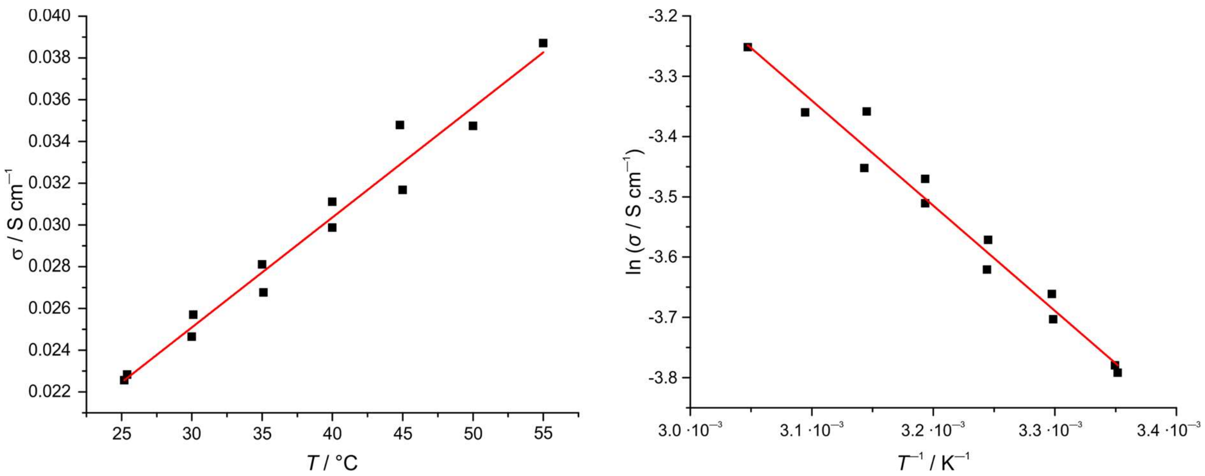

SI Fig. 2: Temperature-dependent electrical conductivity of Cu_3*hhtp*$_2$-MOF coatings on glass slides with linear fits. The activation energy (E_A = 0.15 eV) and bandgap (E_g = 0.30 eV) are calculated from the slope of the Arrhenius plot (right).

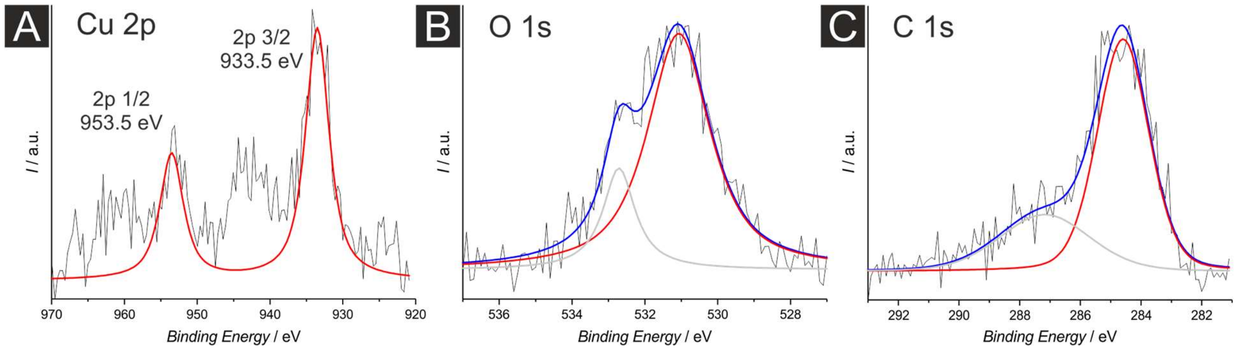

SI Fig. 3: XPS data of Cu_3*hhtp*$_2$ films deposited on gold-coated silicon wafer. Measurements were performed with a pass energy of 20 eV. A) High-resolution Cu2*p* spectrum exhibits only signals for Cu(II) species. B) High-resolution O1*s* spectrum. C) High-resolution C1*s* spectrum.

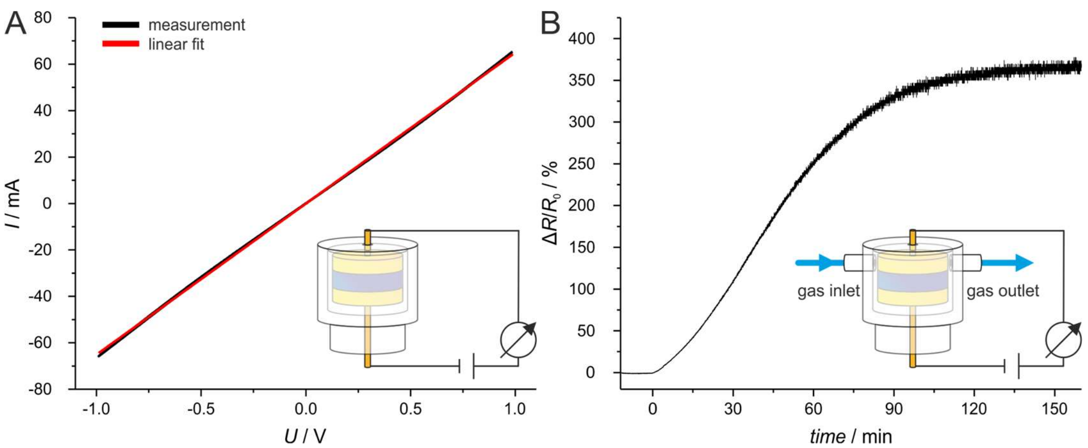

SI Fig. 4: Characterization of the electrical properties measured on pressed pellets of the Cu_3*hhtp*$_2$-MOF in a 2-point setup. (A) Voltage-current curve reveals Ohmic behaviour. (B) Evolution of the resistance when water-saturated argon is passed through the measurement cell at a constant potential of 500 mV.

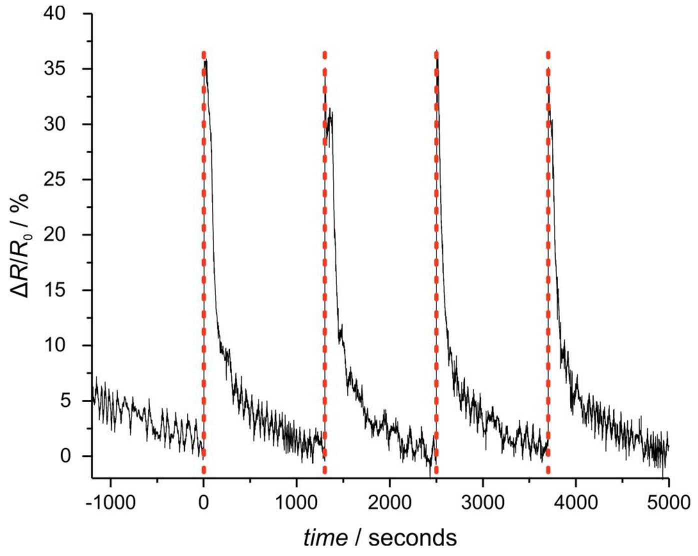

SI Fig. 5: Sensing experiments with Cu_3*hhtp*$_2$-MOF-based coatings on polycarbonate foils, prepared from the nanoplatelets described in this work. Measured changes of resistance of the system coincide with the injection time points (red lines), showing very fast and reversible response to methanol in a passing gas stream.

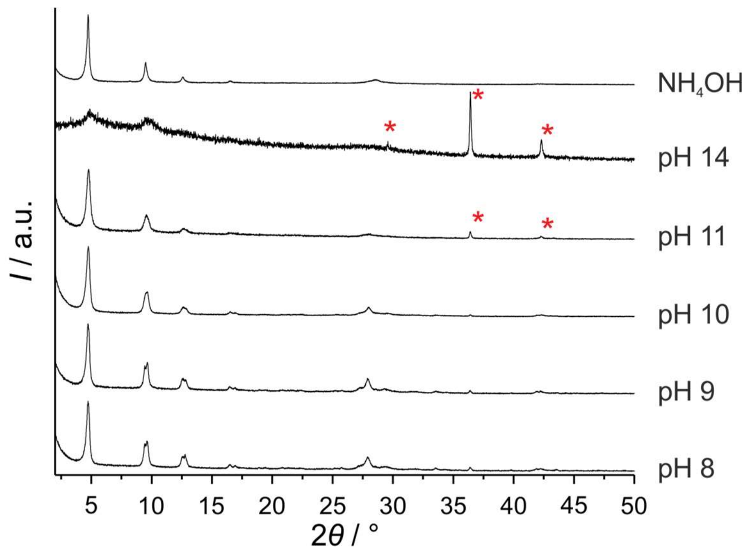

SI Fig. 6: X-ray diffraction patterns of products synthesized at different pH values adjusted by NaOH. Additionally, the NH_4OH-based product is shown for comparison. Marked reflections are related to Cu_2O.

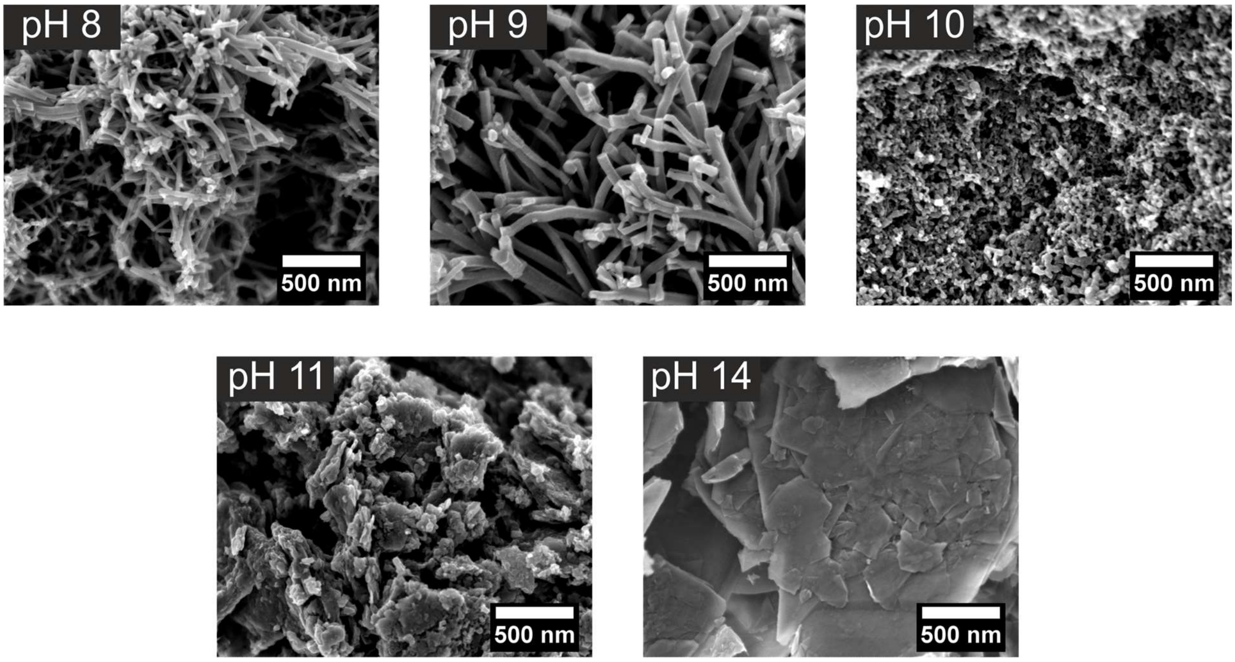

SI Fig. 7: SEM images of products synthesized at different pH values adjusted by NaOH. At lower pH values rod-shaped particles are obtained. Samples prepared at pH 10 and pH 11 show an ill-defined morphology. A sample prepared at pH 14 shows a platelet-like morphology. According to PXRD, this sample consists mainly of copper(I) oxide.

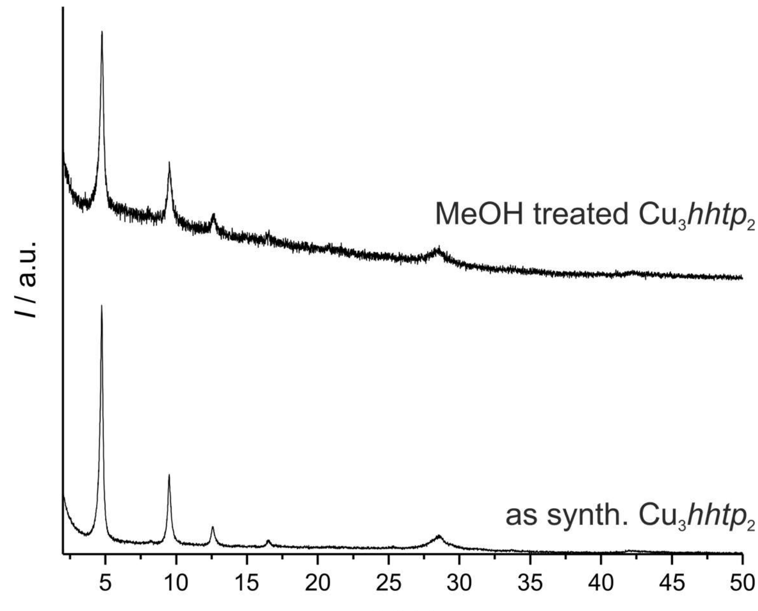

SI Fig. 8: X-ray diffraction patterns of as-synthesized and MeOH-treated Cu_3*hhtp*$_2$. The treatment was performed by stirring the as-synthesized product in methanol for 24 hours. The higher background apparent in the upper PXRD pattern could be ascribed to a slight decomposition of Cu_3*hhtp*$_2$ under these conditions. Note that these conditions are much harsher than those encountered in the methanol sensing experiment where the sample is exposed to only small amounts of methanol in an argon gas stream.